



## Effect of SiC<sub>(p)</sub> Content on the Corrosion Behavior of Nano SiC<sub>(p)</sub>/Cu Composites

M. Abd-Elmonem Metwally <sup>a</sup>, M.M. Sadawy <sup>b</sup>, M. Ghanem <sup>c</sup>, I.G.EL -Batanony <sup>b</sup>

<sup>a</sup> *Egyptian Natural Gas Company (GASCO)*

<sup>b</sup> *Faculty of Engineering, Al-Azhar University, Cairo, Egypt*

<sup>c</sup> *Industrial Education, Suez University, Egypt*

### ARTICLE INFO

#### Article history:

Received on 16 April 2018

Revised form on 10 July 2018

Accepted on 14 July 2018

Available online on 15 October 2018

#### Keywords:

Composite materials,  
SiC<sub>(p)</sub>  
Corrosion  
SiC<sub>(p)</sub>  
Passive film  
Pitting

### ABSTRACT

In this study, the corrosion behavior of ultra-fine Cu and SiC<sub>(p)</sub>/Cu composites powders with different weight percentages of SiC particles was investigated in a simulated sea solution (3.5 wt% NaCl aqueous solution). The composites were produced via powder metallurgy (P/M) route. The corrosion performance was evaluated by immersion tests, electrochemical measurements and SEM. The results reveal that the corrosion performance of SiC<sub>(p)</sub>/Cu composites improved as a function of SiC<sub>(p)</sub> content. The notable increase in corrosion resistance was attributed to the characteristics of protective copper oxide films formed on the surface and decreasing the microgalvanic couple between the reinforcement particles and Cu matrix.

### 1. Introductions

Copper-based alloys have good mechanical performance, formability and thermal conductivity; it also has good corrosion resistance in the marine environment. Copper alloys have long been used for bearing due to their combination of moderate-to-high strength, corrosion resistance and self-lubrication properties [1,2]. The uses and applications of metal matrix composites (MMCs) are in continuous growth, as their properties can be tailored by controlling their constituents: matrix and reinforcement, and method of composite fabrication. The potential of the metal matrix composites (MMCs) is based on the gathering between different properties such as low density,

high stiffness, high strength, wear resistance and intermediate thermal and electrical conductivities. Moreover, the MMCs can provide properties, tailored upon a request, which makes MMCs good candidate for different applications [3]. A great interest has directed towards the fabrication of MMCs reinforced with ceramic particles due to their low cost and the ability to be formed. the powder metallurgy can consider as the most economical solid phase processing route in producing of different mechanical components. P/M provides uniform distribution of reinforcement particles in the matrix with a lower chemical reaction between them [4]. Copper matrix composites reinforced with SiC<sub>(p)</sub> particles combine high electrical and thermal conductivity, enhanced

hardness as well as a low coefficient of thermal expansion (CTE) [4]. The potential applications of this alloy can be further expanded by enhancing its strength. One way to achieve this is to disperse ceramic particles in the metal matrix. Silicon carbide is extensively used as reinforcement particles in MMCs due to its good mechanical and physical properties; it provides high strength, stiffness, good high temperature stability, and oxidation resistance to the matrix material. This alloy is widely used in many environments, where they are being in contact with chloride anions, which significantly affect their corrosion characteristics. However, there is limited information about corrosion behavior of particulate reinforced Cu matrix composites. Therefore, this paper aims to investigate the corrosion characteristics of this alloy matrix that are reinforced with SiC particles in a sea water simulated environment (3.5 wt% NaCl solution).

## 2. Materials and experimental methods

### 2.1. Materials

Cu powder ( 80 nano particle size ) reinforced with silicon carbide particles with average particle size( 90 nano) were fabricated by powder metallurgy. Three different weight percentages (10 wt. %, 20 wt. %, and 30 wt. %) of reinforcement particles were used. The powder was weighed to the required percentages using an electronic balance with an accuracy  $\pm 0.01$  mg. The powder mixtures were vigorously shaken in a completely sealed container to obtain uniform dispersion of reinforcement particles within matrix material particles. Then, the powders mixture was pressed in a high carbon steel compaction die with a diameter of 10 mm and a thickness of 2 cm. Universal testing machine at pressure of 400 MPa was used. The green compacts were placed in oxygen free closed die and sintered at 850 °C for 2 hours.

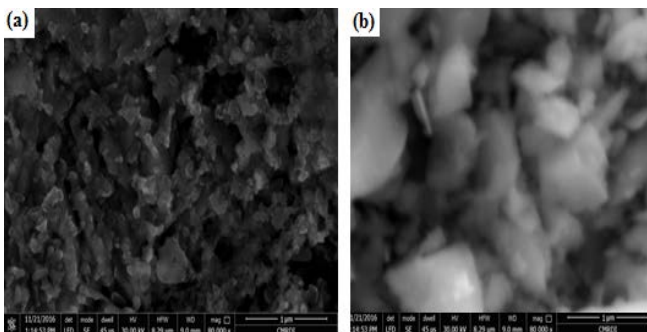


Fig. 1. SEM photomicrograph of morphology of (a) Cu and (b) SiC(p) powders.

### 2.2. Microstructural evaluation

The microstructure of Cu alloy reinforced with silicon carbide particles were analyzed by scanning electron microscope (SEM), model JEOL JSM-6330F at voltage of 20 keV. All samples were prepared by grinding with 350, 600,1000 and 1200 grid SiC(p) paper respectively. After that, these samples were polished using 6,3 and 1 μm diamond paste. The surfaces of samples were cleaned using acetone and dried in air. After that all heat treated samples at different conditions were etched in solution of 5g FeCl<sub>3</sub>+25 mL HCl+50 mL H<sub>2</sub>O.

### 2.3. XRD

The different phases of Cu alloy reinforced with silicon carbide particles before and after corrosion tests were determined using a computer controlled X-ray diffractometer (XRD, Philips Analytical X-ray B.V. Machine) with monochromatic Cu-K radiation ( $\lambda = 0.154$  nm). The scanning range was 25-90 ( $2\theta$ ) with step size of 0.05° ( $2\theta$ ) and counting time of 5 second per step.

### 2.4. Static immersion tests

Static immersion tests were carried out at room temperature according to ASTM G1 and G31. Initially specimens were cleaned in HCl acid solution for 5 minutes, degreased with acetone and washed with distilled water and dried. The initial weights of specimens were taken before immersion using an analytical balance for the original weight (W<sub>0</sub>). After immersion in 3.5 wt% NaCl solutions for 30 days specimens were removed and cleaned with HCl solution for 3 min and dried.

### 2.5. Electrochemical Measurements

All electrochemical experiments were carried out using Potentiostat/Galvanostat (EG&G model 273). M352 corrosion software from EG&G Princeton Applied Research was used. A three-electrode cell composed of SiC(p)/Cu as a working electrode, Pt counter electrode, and Ag/AgCl reference electrode were used for the tests.

Tafel polarization tests were carried out at a scan rate of 0.5 mV/min. The PAR Calc Tafel Analysis routine statistically fits the experimental data to the Stern-Geary model for a corroding system.

The cyclic potentiodynamic curves were obtained by scanning the potential in the forward direction from -250 mV Ag/AgCl towards the anodic direction at a scan rate of 2.0 mV/s. The potential

scan was reversed in the backward direction when the current density reached a value of 0.10 A/cm<sup>2</sup>. After cyclic polarization measurements, all specimens were taken out and dried for microscopic analysis.

All corrosion experiments were carried out in 3.5 wt% NaCl solution as electrolyte. The solutions were prepared from analytical grade and chemically pure reagents using distilled water.

### 3. Results and Discussions

#### 3.1 XRD patterns

The XRD patterns of the SiC(p)/Cu composite with different SiC contents sintered at 850 °C for 2 hours are shown in Fig. 2. The results of XRD data proved that SiC(p)/Cu composites consist of copper and SiC peaks only. It can be said that SiC peaks strengthened gradually with increasing SiC content. Fig. 3. shows the SEM photographs of SiC(p)/Cu composites with different SiC contents. It can be observed that The SiC particles were uniformly distributed inside the matrix and around copper grains.

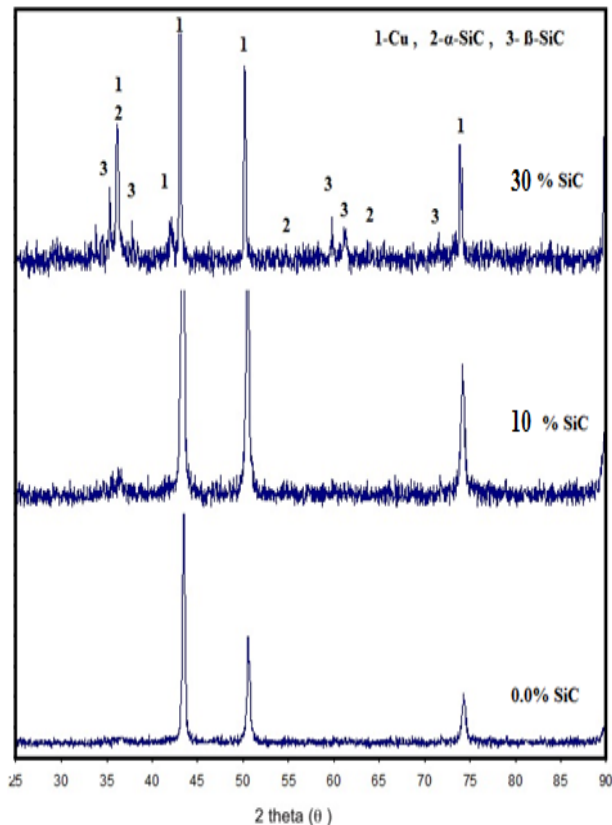


Fig. 2. XRD patterns of SiC(p)/Cu composites with different SiC contents sintered at 850 °C .

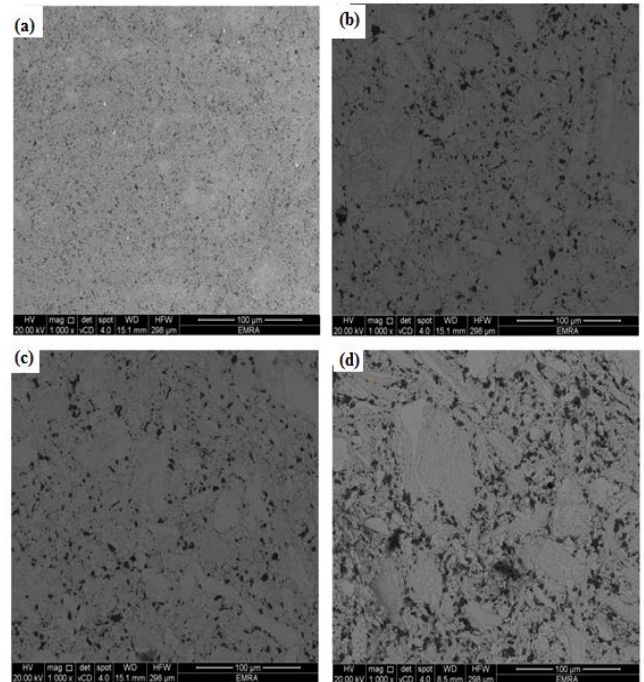


Fig. 3. Microstructure of SiC(p)/Cu composite with different SiC contents sintered at 850 °C . (a) 0.0 wt. % SiC(p) , (b) 10 wt. % SiC(p) , (c) 20 wt. % SiC(p) and (d) 30 wt. % SiC(p) ,

#### 3.2. Immersion tests

The corrosion rate of Cu alloy reinforced with silicon carbide particles is shown in Fig. 4. It can be seen that the corrosion rates of all samples increased as the immersion time increased and attained stable values after 8 days. This attributed to the corrosion layers which formed on the surface of the Cu alloys. These layers acted as a barrier and hampered the ionic transport across the corrosion products and thereby decreasing the corrosion rate. Furthermore, Fig. 4 indicates that the corrosion rate decreases with the increase of SiC content. The observed trend of improvement achieved by adding SiC(p) particles can be attributed to high chemical stability of SiC(p) at the processing temperature during P/M compact specimen fabrications [4]. Therefore, the microgalvanic couple between the reinforcement particles and Cu matrix is reduced.

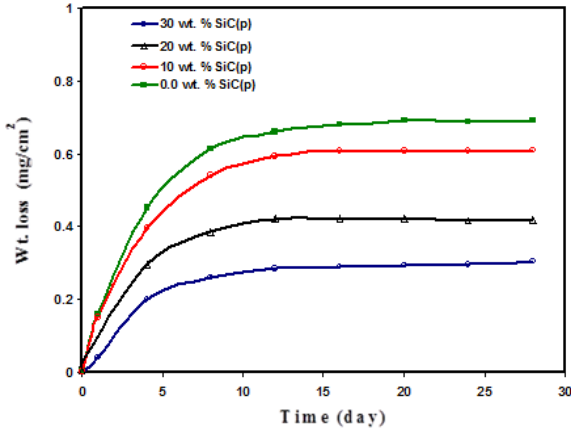


Fig.4 . Weight loss-time curves of SiC(p)/Cu composite with different SiC(p) contents in 3.5wt. % NaCl solution

### 3.3. Tafel polarization

Potentiodynamic polarization curves of Cu alloy reinforced with silicon carbide particles are shown in Fig. 5. All samples were immersed in 3.5 wt. % NaCl solution for about 15 min before polarization tests to achieve their stable OCP values. It is clear that the cathodic and anodic curves of composite samples displays very close polarization behaviour, similar to that of pure Cu powder alloy. The main anodic reaction of Cu in a saline solution is:

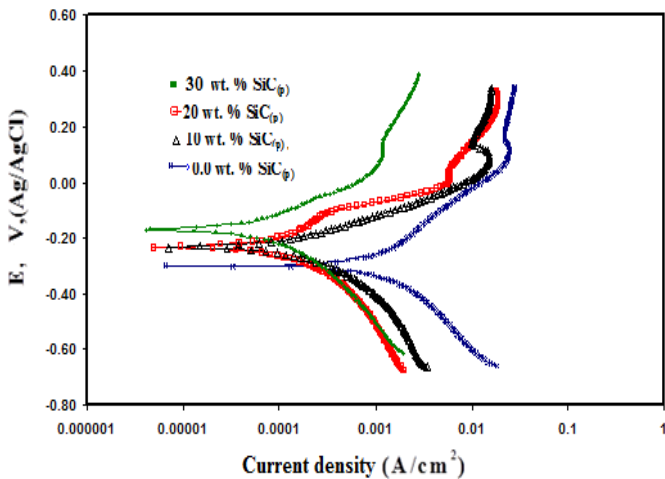
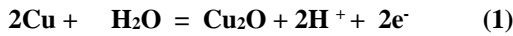


Fig. 5. Tafel polarization curves of SiC(p)/Cu composite with different SiC(p) contents in 3.5wt. % NaCl solution

The electrochemical parameters including corrosion potential ( $E_{\text{corr}}$ ), corrosion current density ( $i_{\text{corr}}$ ), corrosion rate(mpy), anodic and cathodic slopes ( $\beta_a$

and  $\beta_c$ ) were calculated from Tafel plots, and are summarized in Table 1.

Table 1. Electrochemical parameters of SiC(p)/Cu composite with different SiC(p) contents in 3.5wt. % NaCl solution

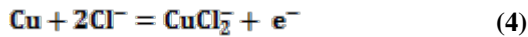
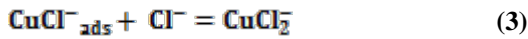
Sample (wt.% SiC(p))	$E_{\text{corr}}$ (mV)	$i_{\text{corr}}$ ( $\text{A}/\text{cm}^2$ )	mpy	$\beta_c$ (mV/dec)	$\beta_a$ (mV/dec)
0.0	-299	$50.32 \times 10^{-6}$	25.4	213	189
10	-220.3	$28.19 \times 10^{-6}$	14.3	199	178
20	-228.1	$16.82 \times 10^{-6}$	8.2	186	145
30	-181.4	$11.56 \times 10^{-6}$	5.6	182	143

It is clear from Fig. 5. and Table 1 that the corrosion current density ( $i_{\text{corr}}$ ) decreases with increasing SiC(p) content. This behaviour may be attributed to the high purity of the SiC(p) reinforcement particles and thus high electrical resistivity of SiC(p) increases. This leads to decreasing the possibility of cathodic reaction occurrence on the surface of these particles. Moreover, the formations of interfacial corrosion products decouple the ceramic reinforcement from matrix alloy [4,5]. Therefore, no chemical reaction between matrix and reinforcement is expected, and the possibility of intermetallic phases formation is very low. All these factors weaken the microgalvanic couple between the reinforcement particles and Cu matrix, leading to reducing the corrosion rate of the composite containing SiC(p) [4, 5]. Also, Fig. 5 and Table 1 indicate that the corrosion potential ( $E_{\text{corr}}$ ) shifts to more noble potential with increasing SiC(p) content in the matrix. The increase in corrosion potential ( $E_{\text{corr}}$ ) value indicates the increase of passivity of alloy due to thick and compact layer of patina formed on the surface. On the other hand, it can be noted that the anodic and cathodic Tafel slopes changed with increasing SiC(p). This means that SiC(p) has obvious effect on anodic and cathodic reactions.

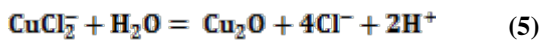
### 3.4. Effect of SiC(p) content on the pitting of Cu matrix composite

To evaluate the effect of SiC(p) content on the passive stability and pitting of Cu alloys in 3.5wt. % NaCl solution cyclic polarization technique was performed. Fig. 6. shows the cyclic polarization curves of SiC(p)/Cu composite in 3.5%wt. NaCl solution. It can be noticed from the cyclic polarization curves that the cathodic polarization curves show a regular pattern and the cathodic current densities decreases with increasing SiC(p) content in the matrix. The anodic curves reveal active, passive, trans-passive and re-passive behaviour. However, the current density in the

passive range decreases with increasing SiC(p) content. This behaviour is due to patina which that acts as a protective coating against further corrosion. The patina layer formed on the surface of SiC(p)/Cu composite involves the following electrochemical steps [6-9]:



The presence of high concentration of  $\text{CuCl}_2$  at the metal surface leads to hydrolysis of  $\text{CuCl}_2$  and the production of  $\text{CuO}_2$  according to [6-9]:



On the other hand, Fig.6. indicates that the reverse anodic curves are shifted to higher currents for all alloys. Therefore pitting is expected for the investigated system in 3.5wt. % NaCl solution. Table 2 summarizes the electrochemical parameters that are extracted from the cyclic polarization curves in sea water. Inspection of the data infers that with the increase in the SiC(p) content, the passive current decreases and the pitting potential ( $E_{pit}$ ) shifts towards more noble direction, implying that a more protective passive film was formed [10]. On the other hand, Table 2 shows that increasing the SiC(p) content has no influence on protection potential.

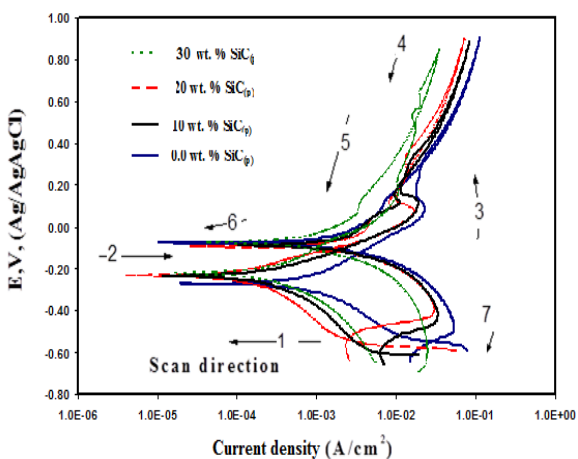


Fig. 6. Cyclic polarization curves of SiC(p)/Cu composite with different SiC(p) contents in 3.5wt. % NaCl solution

Table 2. Cyclic polarization parameters of SiC(p)/Cu composite with different SiC(p) contents in 3.5wt. % NaCl solution

Sample (wt.% SiC(p))	$E_{pas}$ (mV)	$i_{pas}$ ( $\text{A}\cdot\text{cm}^{-2}$ )	$E_{pit}$ (mV)	$i_{pit}$ ( $\text{A}\cdot\text{cm}^{-2}$ )
0.0	-10.4	$3.9\times 10^{-3}$	800	$2.3\times 10^{-2}$
10	-5.2	$3.7\times 10^{-3}$	790	$5.7\times 10^{-2}$
20	2.6	$3.5\times 10^{-3}$	785	$7.2\times 10^{-2}$
30	5.2	$2.9\times 10^{-3}$	780	$8.1\times 10^{-2}$

### 3.5. The electrochemical impedance measurements of

Impedance spectroscopy (EIS) technique was employed to understand corrosion characteristics at metal solution interface. Figs. 7 and 8 indicate Nyquist and Bode curves of SiC(p)/Cu composite alloys in 3.5wt. % NaCl solution. It can be seen that all samples show a capacitive loop in high frequency and a straight line region in low frequency. The straight line region reflects the anodic diffusion process of copper from the surfaces of SiC(p)/Cu composite matrix to the bulk solution and the cathodic diffusion process of dissolved oxygen from the bulk solution to the surfaces of alloys [1,8,11]. The capacitive loop in the high-frequency region can be related to the combination of charge transfer resistance and the double-layer capacitance.

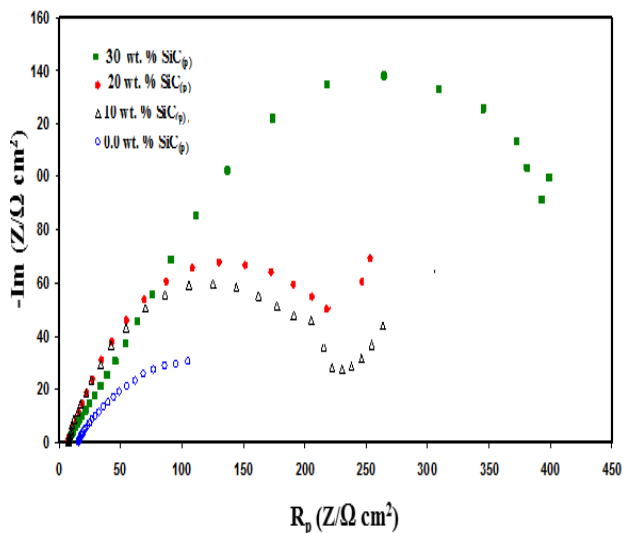


Fig. 7. Nyquist plots of SiC(p)/Cu composite with different SiC(p) contents in 3.5wt. % NaCl solution

The diameter of the semi-circle increases with increasing SiC(p) content as shown in Fig. 7 . The calculated equivalent circuit in Fig. 9 with parameters values for the SiC(p)/Cu composite alloys are listed in Table 3. The equivalent circuit model used to fit the impedance spectra are shown in Fig 8. This model is based on the following equations:

$$Z(\omega) = R_s + Z_s/e(\omega) \quad (6)$$

$$Z_s/e(\omega) = \frac{1}{R_{ct} + Z(w)} + j\omega C \quad (7)$$

where  $\omega$ ,  $R_s$ ,  $Z_s/e(\omega)$ ,  $R_{ct}$ ,  $C$  and  $Z(w)$  are the angular frequency, solution resistance, impedance of solution/electrode interface, charge-transfer resistance, double layer capacitance and Warburg diffusion impedance respectively. In this model,  $Z_s/e(\omega)$  represents the Faradic impedance as a result of the dissolution of Cu species in 3.5wt. % NaCl solution [8].

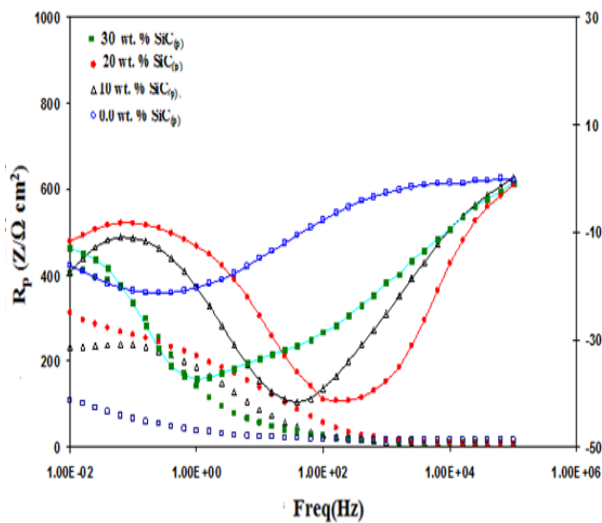


Fig. 8. Bode plots of SiC(p)/Cu composite with different SiC(p) contents in 3.5wt. % NaCl solution

Table 3. Equivalent circuit parameters of SiC(p)/Cu composite with different SiC(p) contents in 3.5wt. % NaCl solution at 25 °C

Sample (wt. % SiC(p))	$R_s$ ( $\Omega \text{ cm}^2$ )	$R_p$ ( $\Omega \text{ cm}^2$ )	$Y_0$ ( $\mu\text{F}$ )	$\alpha$	$W_d$ ( $\text{S s}^{1/2}$ )
0.0	12.2	190	220	0.69	0.04
10	10.1	230	180	0.68	0.03
20	9.1	313	160	0.68	0.006
30	9.2	420	130	0.69	0.008

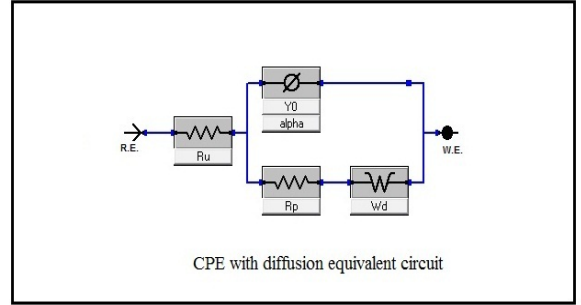


Fig. 9. Equivalent circuit model used to fit the impedance spectra SiC(p)/Cu composite alloys in 3.5wt. % NaCl solution

### 3.6. Surface morphology

Fig. 10(a-d) shows the surface morphology of SiC(p)/Cu composite after cyclic polarization tests in 3.5wt. % NaCl solution. Fig. 10(a) indicates that the patina formed on the surface of the Cu alloy suffers from selective dissolution. This can be attributed to the difference of surfaces crystallographic orientation. On the other hand, Fig. 10(b-d) shows that SiC(p)/Cu composite are corroded uniformly when the aggressive ions attack their surfaces. This is due to the potential difference along surface is very low. Furthermore, the patina formed on SiC(p)/Cu composite exhibits homogeneously compact and smooth passive layer. The XRD pattern (Fig.11) were obtained from the surface of SiC(p)/Cu composite alloys after cyclic polarization tests in 3.5wt. % NaCl solution. The analysis indicates the presence of diffraction peaks of CuCl and Cu<sub>2</sub>O on the surface of SiC(p)/Cu composite. This result is in agreement with equations (2-5).

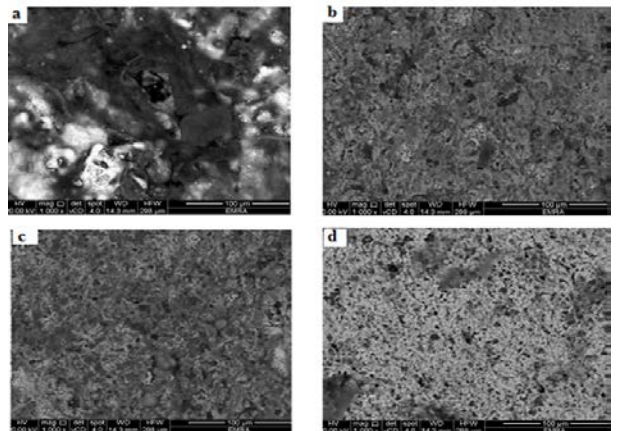


Fig. 10 . Surface morphology of SiC(p)/Cu composite with different SiC(p) contents sintered at 850 °C . (a) 0.0 wt. % SiC(p), (b) 10 wt. % SiC(p), (c) 20 wt. % SiC(p) and (d) 30 wt. % SiC(p)

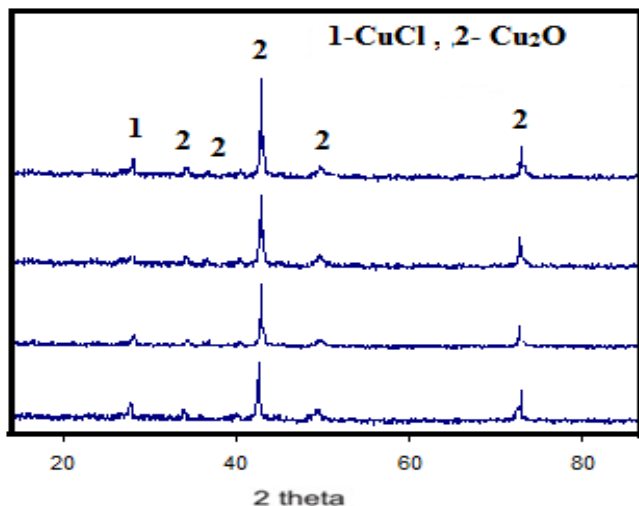


Fig. 11. X-ray diffraction of patina formed on SiC(p)/Cu composite with different SiC(p) contents sintered at 850 °C

#### 4. Conclusions

Effect of nano SiC<sub>(p)</sub> content on the corrosion behavior of SiC<sub>(p)</sub>/Cu composites in 3.5 wt.% NaCl solution. The following main observations are made from this study:

- 1- The corrosion resistance of SiC(p)/Cu composites has been increased with increasing SiC(p) content.
- 2- The uniform corrosion resistance of SiC(p)/Cu composites was enhanced by adding SiC(p) reinforcement particles.

#### 5. References

- [1] K.M. Zohdy , M.M. Sadawy , M. Ghanem, " Corrosion behavior of leaded-bronze alloys in sea water" , Materials Chemistry and Physics 147 (2014) 878-883
- [2] Hu Ming, Zhang Yunlong, Tang Lili, Shan Lin, Gao Jing, Ding Peiling, "Surface modifying of SiC particles and performance analysis of SiCp/Cu composites", Applied Surface Science 332 (2015) 720–725
- [3] A.S. Prosviryakov , "SiC content effect on the properties of Cu–SiC composites produced by mechanical alloying" , Journal of Alloys and Compounds 632 (2015) 707–710
- [4] M. A. Almomani, W. R. Tyfour, M. H. Nemrat , "Effect of silicon carbide addition on the corrosion behavior of powder metallurgy Cu-30Zn brass in a 3.5 wt% NaCl solution" Journal of Alloys and Compounds 679 (2016) 104-114
- [5] T. Kosec a, I. Milosev, B. Pihlar "Benzotriazole as an inhibitor of brass corrosion in chloride solution" Applied Surface Science 253 (2007) 8863–8873.
- [6] A. M. Hosny, M. M. Sadawy, M. Ramadan, K.M. Zohdy, A. A. Atlam, " Effect of heat treatment on corrosion and electrochemical behavior of Aluminum-bronze alloy in 1M H<sub>2</sub>SO<sub>4</sub> solution " 5<sup>th</sup> International Conference on Corrosion Mitigation and Surface Protection Technologies, 2016 : 133-147.
- [7] B. Sabbaghzadeh , R. Parvizi a, A. Davoodi , M.H. Moayed, "Corrosion evaluation of multi-pass welded nickel–aluminum bronze alloy in 3.5% sodium chloride solution: A restorative application of gas tungsten arc welding process", Materials and Design 58 (2014) 346–356.
- [8] M. M. Sadawy and M. Ghanem "Grain refinement of bronze alloy by equal-channel angular pressing (ECAP) and its effect on corrosion behaviour" Defence Technology 12 (2016) 316–323
- [9] D.R. Ni , B.L. Xiao , Z.Y. Maa, Y.X. Qiao , Y.G. Zheng , "Corrosion properties of friction–stir processed cast NiAl bronze", Corrosion Science 52 (2010) 1610–1617.
- [10] M. M. Sadawy and M. Ghanem "the influence of Sn, Zn and Pb on microstructure, mechanical properties and corrosion behavior o leaded-bronze alloys", Al-Azhar University Engineering Journal, JAUES Vol. 9, No. 4, Dec. 2014, 1-10
- [11] A. M. Hosny, "Effect of heat treatment on corrosion and wear of aluminum bronze alloy reinforced with austenitic stainless steel particles" Thesis, Degree M.Sc, Faculty of Engineering, Department of Mining and Metallurgical Engineering, Al-Azhar University, 2017: 1- 96.